Photoluminescence study of the carbon antisite-vacancy pair in 4*H*- and 6*H*-SiC

J. W. Steeds
Department of Physics, University of Bristol, Tyndall Avenue, Bristol BS8 1TL, United Kingdom
(Received 13 May 2009; revised manuscript received 3 September 2009; published 7 December 2009)

Two sets of prominent photoluminescence (PL) lines, called A and B here, in electron-irradiated and ion-implanted 4*H*-SiC have been investigated by low-temperature PL microscopy. From their spectral details, temperature dependence, emission energies, introduction, and annealing characteristics it is concluded that they arise from the neutral on-axis and off-axis carbon antisite-vacancy pairs $(V_CC_{Si})^0$. Photoluminescence excitation spectroscopy has been used to derive an energy-level diagram for the B set of lines of 4*H*-SiC. The creation of these centers is demonstrated as a process that is sensitively dependent not only on the *n* or *p* doping of the material, as has been proposed but also on the temperature and the existence of inhomogeneous internal electric and strain fields. Samples of different purities from many different sources have been studied. Relatively impure, highly compensated doped samples exhibit very strong A and B PL and are referred to as AB material. Purer materials, largely uncompensated, called V here, that are *n*(N) or *p*(Al) doped, have photoluminescence from Si vacancy related defects but relatively little A or B intensity even after annealing at 900 °C. Similar sets of PL lines have also been observed in ion-implanted 4*H*-SiC and electron-irradiated 6*H*-SiC and investigated to a more limited extent. A wide range of different electron-irradiation conditions has been explored.

DOI: 10.1103/PhysRevB.80.245202 PACS number(s): 61.72.J−, 61.82.Fk, 78.55.Hx

I. INTRODUCTION

Intrinsic point defects in 4*H*- and 6*H*-SiC, and complexes derived from them, have been recently the focus of many intensive investigations. They play important roles in controlling the electrical and optical properties of the materials. The current state of understanding has been well reviewed.[1,2] An area of uncertainty concerns Si vacancies, their identification, clustering and transformation into carbon antisite-vacancy pairs. The focus of the most recent work has been on the interpretation of electron paramagnetic resonance (epr) data and of data obtained from related techniques.[2] From this work the epr spectra of $(V_CC_{Si})^+$ and $(V_CC_{Si})^-$ have been established.[2] However, as the techniques used rely on the nonzero spin of the defect being studied they do not detect its neutral state. Photoluminescence spectroscopy lacks some of the useful properties of epr that make defect identification possible by that technique, but has others that can be exploited to study defects lacking spin with great sensitivity. By taking advantage of some of these other properties, in particular, the ability to measure the energy of local vibrational modes accurately, we have recently been able to identify some C-interstitial-related defects in 4*H*-SiC, including one that exists in two very similar forms, one with spin the other without.[3] In the present work we make use of the special properties of microscopic low-temperature PL spectroscopy to identify the neutral V_C-C_{Si} defect and to investigate its formation in 4*H*- and 6*H*-SiC. It has been demonstrated by theoretical work that the Si vacancy is unstable against transformation into the V_CC_{Si} defect, particularly in the case of *p*-type material.[4] We shall show that there exists a very subtle and delicate relationship with not only the Si vacancy but also with other irradiation-induced defects and that the stability of the Si vacancy depends on other factors in addition to the nature of the doping of the material.

II. EXPERIMENTAL DETAILS

The samples studied were mainly electron irradiated but some ion implantations were also carried out. All of the electron irradiations were performed on bulk specimens, mostly with epilayers, but some without, mainly using transmission electron microscopes (TEMs). A specially adapted Phillips EM 430 TEM was used for the large majority of the electron irradiations. It had a dog's-leg introduced into its linear accelerator to ensure ion-free electron beams. This instrument had sample temperature control from 20 to 1300 K and continuous control of the accelerating voltage from 50 to 300 keV. The vacuum in this microscope was ion pumped and the beam current was monitored before and after the irradiations. 600 and 800 keV irradiations were performed at the National Center for Electron Microscopy in Berkeley CA and at 1 MeV at the Max Planck Institute in Stuttgart. One sample was irradiated with 1.5 MeV electrons in a commercial accelerator. The ion implantations were carried out at the Ion Beam Centre at the University of Surrey. One of the reasons for using TEMs was the ability to create damage in several well-defined and preselected regions of a sample. By use of condenser lenses it was possible to deliver the electron beam in the form of a top-hat profile of uniform intensity of chosen diameter with a sharp cutoff at the periphery. Details of the intensity profile are given elsewhere.[5] Typical diameters of 100–200 μm were used. The ion beams were of 1 MeV protons or He ions focused to a probe of approximately 5 μm diameter.

Subsequent investigation was mainly carried out with one or other of two Renishaw micro-Raman spectrometers fitted with Oxford Instruments cryogenic stages that achieved temperatures of about 7 K with liquid He cooling. One of these was operated at 325 nm with a He/Cd laser, the other was operated at 488 nm with an Ar ion laser. The spatial resolution of the 325 nm system was ~2 μm and that of the 488

TABLE I. Details of the N-doped samples studied extensively in this investigation. The epilayers were all *n*-type apart from the sample marked † which was supplied as a high-purity semi-insulating material. The substrates were all highly conducting and N doped in the range $5-9\times10^{18}$. nd signifies that N was not detected.

N doping concentration (cm^{-3})	Al/N intensity ratio	Epilayer thickness (μm)	Type
2×10^{13}	Al nd	15	V
3.5×10^{13}	Al nd	80	V
8×10^{13}	0.03	40	V
5×10^{14}	0.11	30	V
7×10^{14}	0.02	25	V
10^{15}	0.02	35	V
10^{15}	0.03	10	V
$2.5\times10^{15\dagger}$	0.03	$\gtrsim$180	AB(V)
5×10^{16}	0.05	$\sim$10	V
6×10^{17}	0.03	10	V

TABLE II. Details of the Al-doped samples studied extensively in this investigation. The epilayers were all *p*-type without DAP PL and approximately 30 μm in thickness. They were grown on substrates that were all highly conducting and N doped in the range $5-9\times10^{18}$.

N_A-N_D carrier concentration (cm^{-3})	N/Al intensity ratio	Type
2.5×10^{15}	0.15	V
5.5×10^{15}	0.4	V
7×10^{15}	0.24	V
1.3×10^{16}	1.4	V
2×10^{16}	0.02	V
2.5×10^{16}	1.4	V
4×10^{16}	0.02	V
4×10^{16}	N nd	V
4×10^{19}	N nd	V

nm system was 1 μm. The samples were studied in back-reflection mode with the irradiated face, mostly (0001), perpendicular to the incident laser beam or with the sample mounted so that the laser beam was incident perpendicular to the usual direction of electron irradiation, with the laser polarization either perpendicular or parallel to [0001]. Photoluminescence excitation spectroscopy experiments were performed at 2 K at the University of Stuttgart using a dye laser or a Ti-sapphire laser. PL lifetime measurements were performed with liquid helium cooling both in Bristol and at the University of Stuttgart. Low-temperature (4.2 K) PL measurements were performed at magnetic fields up to 12T at the High Field Facility in Grenoble.

Annealing of the samples was mostly performed in a Linkham mini furnace under a N atmosphere but some annealing was performed in the ion-pumped TEM. These both had rise and fall times of a few minutes. The time at temperature was 0.5 h. No differences in results were detected between these two methods. Annealing at temperatures above 1050 °C was carried out at the University of Newcastle in a specially designed furnace.

A very wide range of 4*H*-SiC samples was studied from a number of different sources. These included *n*(N)-, *p*(Al)-type, and semi-insulating material. Details of the 4*H*-SiC samples on which this report is mainly based are given in Tables I–III. Each of these was subjected to a range of different irradiation conditions and annealing treatments. The substrates of all the samples in Tables I and II gave very broad spectra in the bound exciton region typical of their N-doping levels. The samples in the tabulations are those for which most background information was available, such as epilayer thicknesses, doping levels and conductivities. However, a few additional samples similar to those in Table I were also studied. The substrates of the samples in Table III exhibited rather similar donor-acceptor pair (DAP) emission to that from their epilayers. The intensity ratios given in the table are those of the N and Al bound exciton peak heights to the DAP intensity maximum at about 420 nm for [0001] laser incidence. Several bulk materials were also studied that had weaker DAP emission with N peaks having comparable intensity levels. They were of unknown conductivity and the N/DAP ratios varied considerably from one region of the samples to another. The results obtained from these were intermediate between the AB and V types that are to be described. The 6*H*-SiC samples studied were mainly of bulk materials or of relatively thin epilayers of unknown thickness and background information about them was lacking. Apart from information provided by the suppliers (mainly electrical characterization) they were characterized for this study by Raman spectroscopy, obtaining, where possible, local electron concentrations of *n*-type material by measurements on the high-energy longitudinal optic (LO) mode, and by low-

TABLE III. Details of the samples exhibiting strong DAP PL studied extensively in this investigation. The spectra were obtained with approximately 30 W/cm^{-2} 325 nm laser intensities. They were similar in form to the spectrum c of Fig. 2 of Ref. 6 and the DAP intensity was measured at its maximum at about 420 nm. Note that the relative peak heights of the N and Al bound-exciton peaks varied considerably. No information is available about the substrate doping of the first two samples and the last sample but these samples, as well as three others that behaved similarly on irradiation, gave strong substrate DAP PL with approximately equal N and Al bound-exciton peaks. The sample with a † was provided as semi-insulating (na signifies not applicable).

Doping of epilayer (cm^{-3})	N/DAP peak-height ratio	Al/DAP intensity ratio	Epilayer thickness (μm)	Substrate doping (cm^{-3})	Type
$p10^{15}$	0.18	0.03	30		AB
$p\sim10^{16}$	0.17	0.11	$\sim$10 μm		AB
$p2.9\times10^{16}$	0.065	0.33	10	9×10^{17}	AB
Semi-insulating	0.22†	0.06	$\gtrsim$100	na	AB
$p\sim10^{16}$	0.004	0.004	$\sim$10 μm		AB

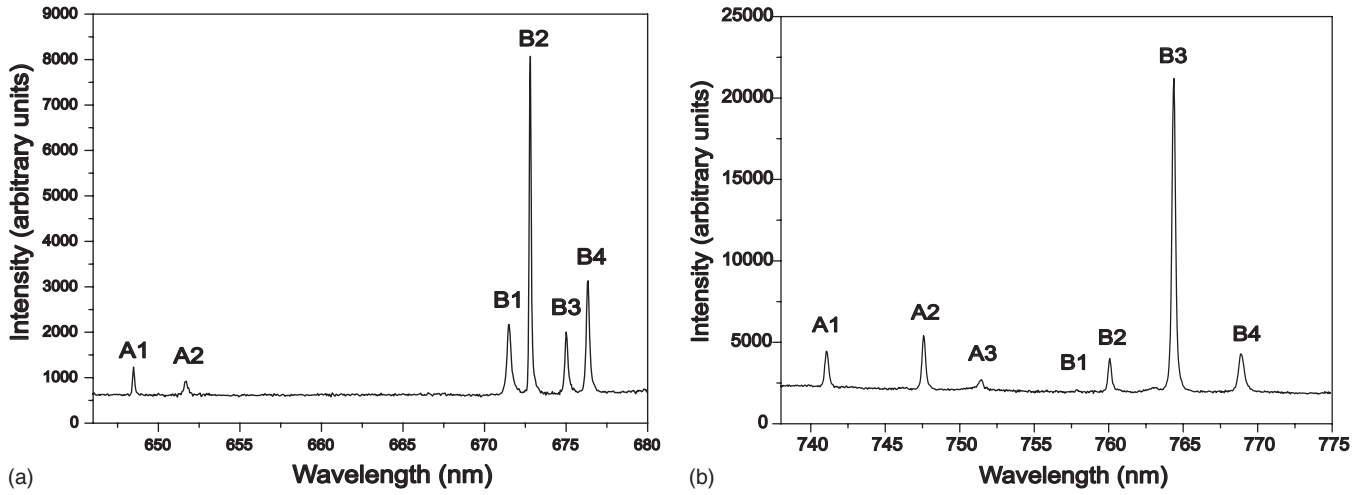

FIG. 1. (a) AB spectrum of 4*H*-SiC collected with the sample edge on to the laser and with a polarizer to select the electric field parallel to [0001] thus enhancing the A2 and B1 lines relative to the others. (b) AB spectrum of 6*H*-SiC with the laser incident along [0001]. 488 nm excitation at ~7 K.

temperature photoluminescence PL spectroscopy to reveal the bound exciton or DAP luminescence.

The *n*-type material varied in N content from $10^{13}-10^{19}$ cm^{-3} and the *p*-type material varied in Al content from $10^{15}-10^{19}$ cm^{-3}. The purest *n*-type material had no evidence of Al bound-exciton PL but most of the *n*-type materials with doping levels above 10^{15} cm^{-3} had small amounts of Al present according to this criterion. However, the *p*-type material was more variable in nature. Some of the samples studied had Al concentrations up to 4×10^{19} cm^{-3} without any hint of N-bound exciton PL. Others had significant levels of N-related PL without any DAP PL. Yet others in the $10^{15}-10^{16}$ cm^{-3} doping range (Table III) were evidently highly compensated with strong and well-resolved DAP PL. The semi-insulating samples had been supplied for high-energy particle detection.

Four ^{13}C enriched samples were studied, three with nominally the same degree of ^{13}C enrichment (~50%) and one with a lower level of enrichment (~30%). These are not included in the tables, were sublimation grown, without epilayers, and were found from PL studies to have N contents ~10^{18} cm^{-3} but as they lacked plasmon coupling to the Raman LO mode it is concluded that they were of low conductivity.

A smaller number of 6*H*-SiC samples was studied and none of these had epilayers thicker than 10 μm. Some of the samples were bulk grown without epilayers. As the epilayers were not found to contribute significantly to the PL spectra in comparison with their substrates our present results are mainly from bulk material with consequently relatively poor quality control and uniformity. Commercial samples of 4*H*- and 6*H*-SiC were purchased from Cree.

III. EXPERIMENTAL RESULTS

A. General introduction

During the course of examination of a wide range of electron-irradiated samples of 4*H*-SiC, over several years, it was found that most of the results exhibited remarkable consistency and showed systematic trends with controlled changes in irradiation conditions. However, it has now become apparent that there is a significant difference between the samples of 4*H*-SiC that have been obtained from different sources. At one extreme, the irradiated samples emitted at 1.439 eV (861.3 nm) under 488 nm laser excitation, PL that is frequently referred to as the V_1 center and has been associated with single isolated Si vacancies.[7] Such samples will be referred to as category V here. At the other extreme, there was little or no detectable V_1 PL under 488 nm excitation (there is evidence that situation may be changed with 785 nm excitation) but instead very strong PL emission occurred with zero phonon lines (ZPLs) in the wavelength range 645–680 nm. A small number of samples exhibited significant PL intensity from both of these spectral systems. Less complete studies of similarly irradiated 6*H*-SiC revealed, in addition to V_1 PL, a set of ZPLs in the wavelength range 745–780 nm that had several common characteristics to those of the AB PL in 4*H*-SiC. Typical spectra from the two polytypes are shown in Fig. 1. The AB emission lines occurred in two groups which will be referred to as A (A1, A2 in 4*H*; A1, A2; and A3 in 6*H*) and B (B1, B2, B3, and B4). The B1-B4 emission from both polytypes had relatively strong vibronic coupling with gap modes but without local vibrational modes. The individual lines tended to have asymmetric profiles, tailing off on their long wavelength sides. The A series of lines was often considerably weaker than the B series and both exhibited marked thermal stability on annealing as detailed later. Their emission energies scaled approximately with the band-gap energies of the two polytypes. With 325 nm excitation it was not possible in most cases to find AB PL from either category of material but no significant differences in their alphabet line emission[8] were detected.

V_1 emission has been the subject of several previous publications[7,9,10] but there has not yet been a systematic study reported for the AB emission nor has there been, apart from a preliminary report,[11] any attempt to account for its apparent anticorrelation with V_1 centers. Here we shall not

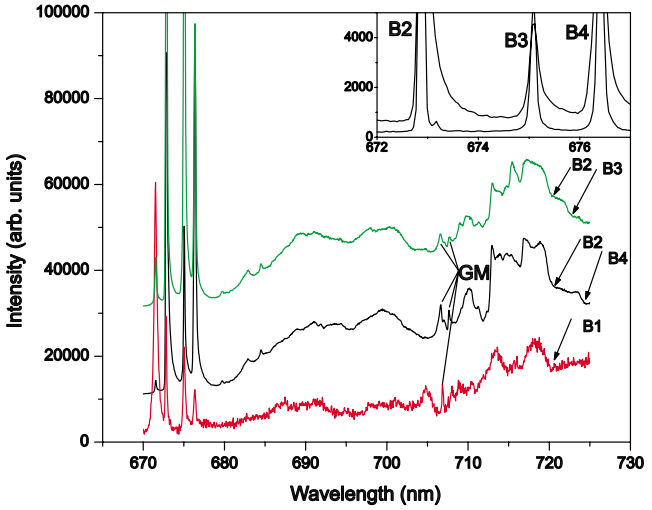

FIG. 2. (Color online) B1-B4 spectra from 4*H*-SiC, displaced vertically for convenience, recorded at different sample temperatures and polarizations so as to change the relative intensities of the individual contributions to the spectrum. The upper two spectra were obtained without a polarizer but the lowest spectrum was obtained with the electric field parallel to [0001]. The top and bottom spectra were obtained at about 40 K to enhance the intensities of B1 and B3 relative to B2 and B4. The middle spectrum was obtained at about 10 K. Gap modes are marked GM. The arrows indicate the first-order limits of bulk phonon contributions to the vibronic structure. The inset to the figure (with axes as for the main figure) shows the intensity profiles of the individual lines for regions having undergone very different doses of irradiation. The sharper lines were obtained from a lower dose (10^{18} e cm^{-2}) region of an epilayer sample and the broader lines from a higher dose region (10^{20} e cm^{-2}) of a substrate. It is notable that in the sharper case the B2 line has a second-intensity maximum at a slightly longer wavelength. The broader lines exhibit strong asymmetry. 488 nm excitation at ~7 K.

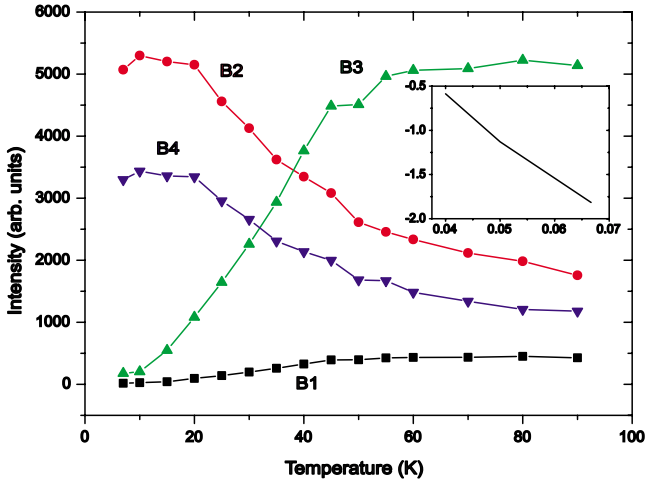

FIG. 3. (Color online) Temperature dependences of the intensities of the B1-B4 lines. In the inset, the ordinates are $\ln(I_{B3}/I_{B4})$ and the abscissae are reciprocal absolute temperature.

only undertake a detailed examination of these optical centers but also relate our results to properties of other well-known optical centers that are created in these materials by electron irradiation in attempting to account for the observed annealing behavior. We then produce evidence to support the identification of the centers responsible as nearest-neighbor neutral carbon vacancy (V_C) carbon antisite (C_{Si}) pairs and discuss the reasons for the differences between the V and the AB behavior.

B. Properties of the AB emission of 4*H*-SiC

The A and B emissions of 4*H*-SiC invariably occurred together, the A emission being considerably weaker as shown in Fig. 1 (see also Fig. 4). The emission wavelengths (energies) of the ZPLs were as follows: A1—648.5 nm (1.911 eV), A2—651.7 nm (1.902 eV), B1—671.6 nm (1.846 eV), B2—672.85 nm (1.842 eV), B3—675.1 nm (1.836 eV), and B4—676.4 nm (1.832 eV). Figure 1 also shows the equivalent spectrum of 6*H*-SiC for comparison. The characteristic four-line spectrum of the B1-B4 emission is illustrated in more detail in Fig. 2. The individual B1-B4 lines each had a similar asymmetric profile, with a long-wavelength tail. The sharpest spectra, obtained at relatively low doses, revealed that the form of B2, at least, involved a much weaker subsidiary peak at a slightly longer wavelength (see inset to Fig. 2). The spectra had a characteristic vibronic structure that is contributed to by all the no-phonon lines. This conclusion, illustrated in Fig. 2, was arrived at by setting up conditions that changed the relative intensities of the no-phonon peaks. The figure shows spectra, displaced vertically for convenience, generated with the sample edge-on selecting light polarized parallel to [0001] to accentuate B1 (bottom curve), for normal incidence at 80 K to accentuate B3 (middle curve) and at ~7 K to accentuate B2 (top curve). The spectra exhibit gap modes [gap mode (GM) in the figure] but no local vibrational modes of higher energy than the propagating modes.

The temperature dependence of the B spectrum, (Fig. 3), reveals that it is composed of two pairs of lines, B1 and B3, B2 and B4. By recording the spectra at a series of different temperatures it was found that the lines B1 and B3 became rather weak at about 7 K, the normal temperature of our experiments. At 2 K (in Stuttgart) only B2 and B4 were detected. Analysis of these results was performed on the basis of Boltzmann statistics and showed approximately linear relationships between the relevant intensity ratios and reciprocal absolute temperature (see the inset to Fig. 3). The thermal activation energy deduced in this way was 4.2 meV. This should be compared with the energy differences between B1 and B3, B2 and B4, which are both 3.6 meV indicating that B1 and B3 are thermally populated excited states associated with B2 and B4, respectively. In fact, the relative intensities of the B1-B4 lines acted as a convenient measure of the temperature attained in our experiments. The relative intensities of the A lines did not change significantly with increase in temperature. The individual lines broadened and became more asymmetric as the temperature was raised.

The breadth of the individual lines varied considerably. Low doses gave narrower, less-asymmetric line profiles (inset to Fig. 2) and the A1 and B2 lines were then somewhat narrower than the others. The linewidths and asymmetry in-

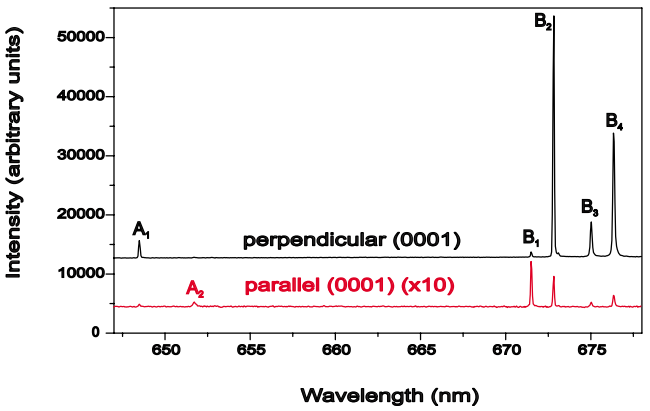

FIG. 4. (Color online) B1-B4 spectra from 4*H*-SiC, displaced vertically for convenience, obtained with the sample mounted edge on to the incident laser beam. 488 nm excitation at ~7 K.

creased considerably with increase in electron dose and with the temperature at which the spectra were recorded. By mounting the samples edge on, so that the incident laser beam was perpendicular to [0001], the polarization of the emission lines was investigated. Samples were mounted edge on with the polarization of the incident laser beam both parallel to and perpendicular to [0001] but these two different configurations gave similar experimental results. As illustrated in Fig. 4, A2 and B1 are partially polarized parallel to [0001] but A1, B2, B3, and B4 are primarily polarized perpendicular to [0001].

Spectra have been obtained from samples containing approximately 30% of ^{13}C of 4*H*-SiC and these exhibited a shift of the vibronic part to shorter wavelengths as expected because of the involvement of heavier atoms. Figure 5 shows a comparison of a spectrum from a ^{13}C enriched sample with that from a sample with natural abundance of carbon isotopes. It is apparent that the ZPLs of the enriched sample are

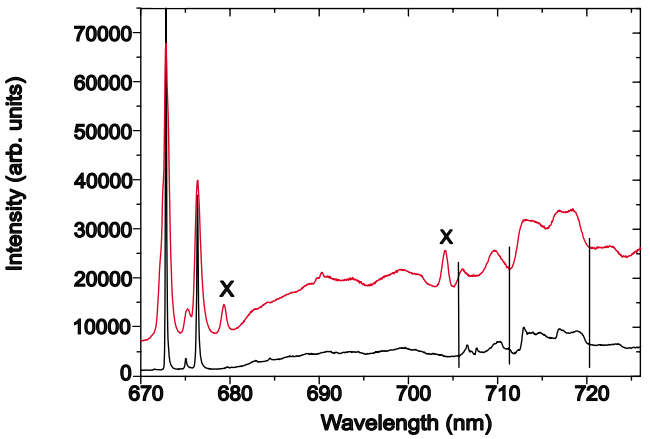

FIG. 5. (Color online) B1-B4 spectra obtained at approximately 7 K from one sample with a natural abundance of C isotopes (lower curve) and another with approximately 30% ^{13}C enrichment (upper curve) and displaced vertically for convenience. The vertical lines are added as a guide to the spectral shifts caused by the isotopic replacement. The spectrum from the ^{13}C enriched sample is broadened considerably and has extraneous spectral features marked X. 488 nm excitation at ~7 K.

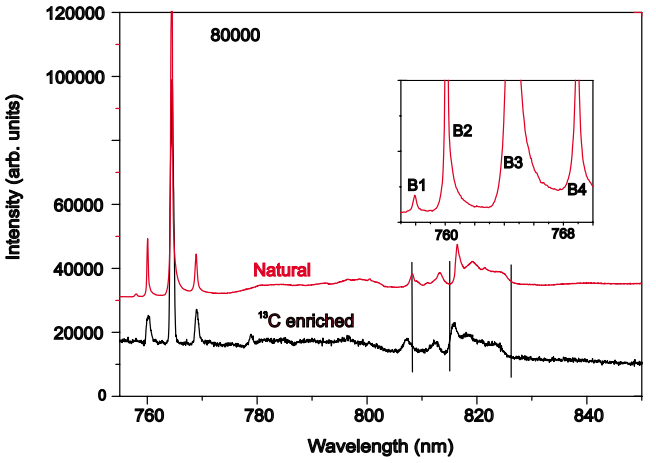

FIG. 6. (Color online) Four-line spectra of 6*H*-SiC that are the equivalent of the B1-B4 spectra of 4*H*-SiC. One spectrum (displaced vertically for clarity) was generated from a sample with natural abundance of C isotopes and the other from a sample with about 50% of ^{13}C, as indicated. The vertical lines have been added as aids to revealing the shifts introduced by the isotopic replacement. The inset shows the ZPLs of the natural sample with sufficient enhancement to reveal B1. 488 nm excitation at ~7 K.

broader than those of the other sample, an effect similar to that of broadening with increase in dose, and caused by inhomogeneous nanoscale fields induced by the mixture of carbon isotopes in the ^{13}C enriched sample. In addition, careful examination of this spectrum reveals a small twofold splitting of the ZPLs and this is believed to be the result of the isotopic replacement with the shorter wavelength component being associated with the ^{13}C, a point discussed in more detail below.

Measurements of the decay of B2 PL intensity with time after excitation yielded a lifetime of 0.27 μs at about 2 K. Neither splitting nor shift of the ZPLs was detected in magnetic fields up to 12 T.

C. Properties of the AB emission of 6*H*-SiC

A typical spectrum of the AB emission from 6*H*-SiC is shown in Fig. 1. For this polytype there were three A ZPLs, not two as for 4*H*-SiC, and their intensities relative to the B ZPLs were considerably more variable. The emission wavelengths (energies) of the ZPLs were A1—741.1 nm (1.672 eV), A2—747.6 nm (1.658 eV), A3—751.5 nm (1.650 eV), B1—757.9 nm (1.635 eV), B2—760.1 nm (1.631 eV), B3—764.4 nm (1.621 eV), and B4—768.9 nm (1.612 eV). Note that the B1 line is not evident in Fig. 1(b) because it is much lower in relative intensity for [0001] laser incidence but is clearly visible in the inset to Fig. 6 and for perpendicular laser incidence. As in the case of 4*H*-SiC, the width and asymmetry of these lines was dependent on the defect density, the electron dose and the temperature of recording the PL spectrum. The A1, B2, and B3 lines were somewhat narrower than the others.

Although there were again four B lines (Fig. 6) the nature of these lines was different in this case. One major difference was that the relative intensities of this set of lines did not

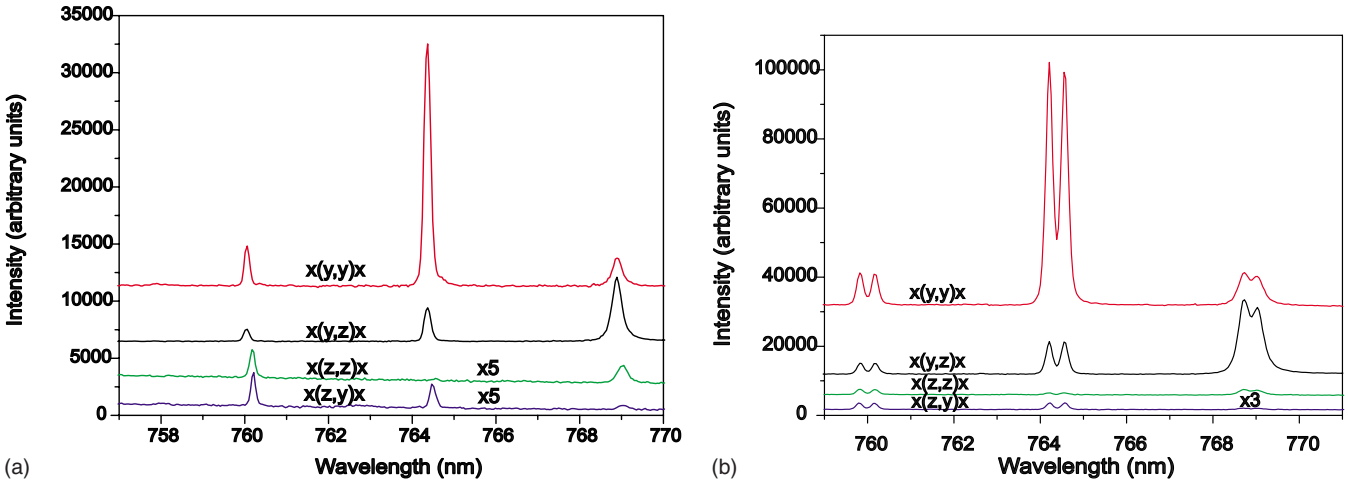

FIG. 7. (Color online) Polarization dependence of the B2-B4 PL lines at ~7 K. The 488 nm laser beam was incident perpendicular to [0001] and its polarization and that of the collected light are given in the Porto notation. The z direction was [0001] and the x and y axes are perpendicular to it and to each other. Figure (a) is for a natural sample and (b) for the (split) B2-B4 PL lines for a 50% ^{13}C enriched sample. The two lowest spectra have been increased threefold in relative intensity and the spectra are displaced vertically for clarity.

change significantly on raising the temperature of observation. Another was that the first-order vibronic spectra were terminated at a single wavelength corresponding to an energy difference from the main (B3) line of the maximum bulk phonon energy. This situation should be compared with that shown in Fig. 2 where a series of different terminations are evident. A further significant difference is that, unlike the results from 4*H*-SiC, the edge on results from 6*H*-SiC were found to depend on the polarization of the laser beam relative to the crystal orientation, the intensity of some of the lines being considerably enhanced when the polarization of the excitation and emission were parallel to each other. The Porto notation[12] has therefore been used to specify the collection conditions [Figs. 7(a) and 7(b)].

In samples with ^{13}C isotopic enhancement, changes to the vibronic structure of the B1-B4 lines occurred that are a consequence of the incorporation of atoms of higher mass (Fig. 6). Much more dramatic and significant is the fact that each of the A and B sets of lines was doubled [Figs. 7(b) and 8). The relative intensities of the lines in each split pair depended on the ^{13}C/^{12}C ratio, the intensity of the shorter wavelength component increasing with the ^{13}C concentration. For approximately 50% of each isotope the intensities were nearly equal but for a sample with 30% of ^{13}C the shorter wavelength line of the pair was reduced considerably in intensity. However, the magnitude of the splitting was independent of this ratio and of the laser position in the irradiated region from which the spectrum was acquired. The splitting is therefore different from the stress related results to be discussed and each line of the split pair corresponds to one of the two different isotopes present in significant quantities. A related but smaller splitting was observed for 13C enriched 4*H*-SiC.

D. Stress-induced splitting of ZPLs

It was not uncommon to encounter splittings of the individual spectral lines obtained from samples without ^{13}C enrichment. This is a typical characteristic of defect centers that are relatively soft such as when a vacancy is involved. Unlike the isotope-induced splittings, when these occurred in samples with natural isotope abundances, the splitting generally varied markedly and systematically with the position of the laser beam on the sample, for example, in the vicinity of a surface crack, although the cause of the stress was not always apparent as in the example illustrated in Fig. 9 where several irradiations were applied to adjoining regions with defined geometries of material processed to fabricate electronic devices. Another particularly clear case was observed for a sample with a 5-μm-thick epitaxial layer of GaN grown on its surface. The epilayer was evidently in a state of biaxial tension with regular cracks along directions making angles

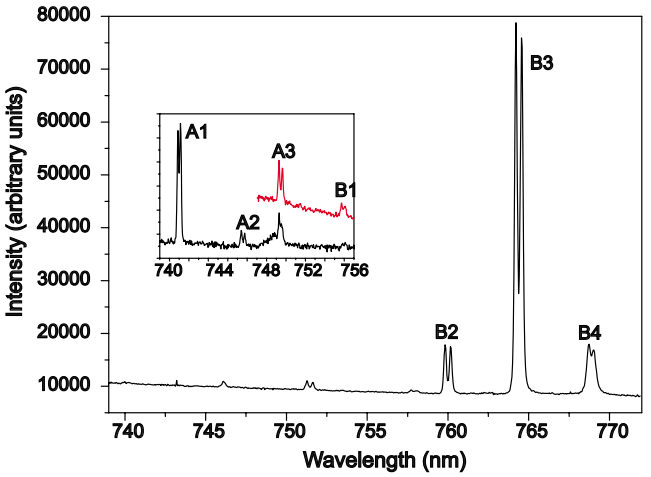

FIG. 8. (Color online) Full AB spectrum of a 50% ^{13}C/50% ^{12}C sample for laser incidence along [0001]. The inset shows details of A1, A2, A3, and B1 lines of the PL spectrum with expanded intensity scales (axes as for the main figure). The upper spectrum in the inset (red online, shifted vertically for clarity) is from the main spectrum below, the spectrum below it (black) is from another region of the same sample. 488 nm excitation at ~7 K.

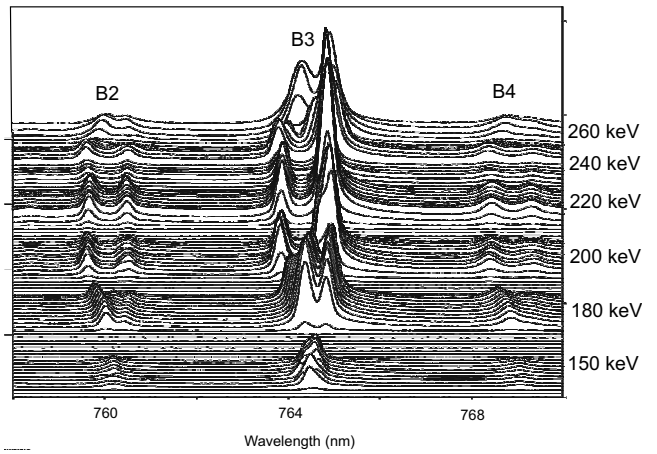

FIG. 9. Spectra generated with 15 μm spacing along a line through five separated irradiated areas, each 150 μm in diameter, at a series of different electron energies, as indicated on the right-hand side. The 6*H* sample used had experienced an unsuccessful attempt at device fabrication and had been N implanted and annealed at 1500 °C in rectangular regions prior to electron irradiation. The strain-induced splitting of the B2, B3, and B4 lines, induced by the device structures, is very clear.

of approximately 60° with each other. The biaxial tension in the GaN away from the cracks was measured by Raman spectroscopy as 0.6 GPa. After electron irradiation the A and B lines observed from these samples were split to some extent everywhere. From these observations it is possible to draw the important conclusion that the A and B lines are very sensitive to stress as well as to ^{13}C substitution. This conclusion is consistent with the line broadening described above. When stress splitting occurred it was mostly twofold in nature for each of the emission lines, with variable relative intensities of the two

lines of each split pair (Fig. 10). Occasionally, threefold splitting was encountered, as in the example from 6*H*-SiC in Fig. 11. As may be seen in this figure, although the line profiles of each individual split line varied it appears that, taking account of broadening, the split lines formed groups with similar splitting properties. The B4 line of 6*H*-SiC was always significantly broader than the others. The relative intensities of the split lines were not found to be temperature dependent. The sensitivity of the A and B lines to stress was another of their notable features.

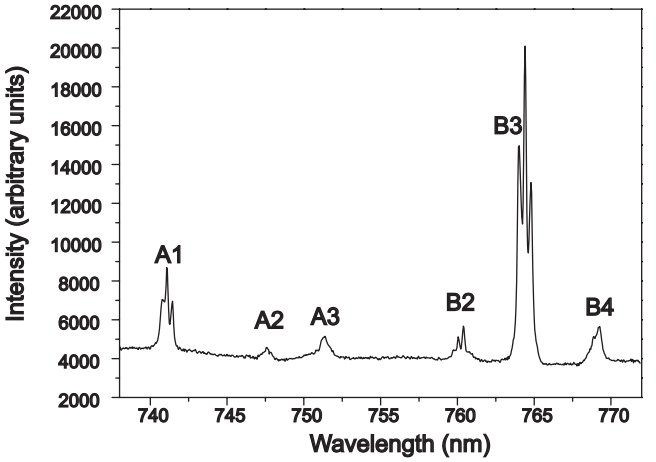

FIG. 11. Threefold stress-induced splitting of the A and B lines from a sample of 6*H*-SiC. A1 and B3 show this splitting clearly, A2, A3, B2, and B4 are broadened by different amounts disguising the effect. 488 nm excitation at ~7 K.

E. Excitation of the B spectra

In order to arrive at a better understanding of the nature of the emission lines, photoluminescence excitation (PLE) spectroscopy experiments have been performed at 2 K by detecting the vibronic structure of the B1-B4 emission as the excitation wavelength was changed. As shown in Fig. 12(a), strong enhancement of the vibronic structure associated with the B emission of 4*H*-SiC was found at three separate wavelengths by tuning a dye laser through the relevant range of wavelengths. There are several interesting aspects of this result. First, resonant excitation occurred at the strongest emission wavelength (672.8 nm) and also at 671.6 nm which was earlier (see Sec. III B) identified as the wavelength of emission from a higher excited state of B2. Even stronger excitation occurred at 664.7 nm (1.865 eV) where no emission had been detected. There was no excitation enhancement at the B4 emission wavelength. The results for 6*H*-SiC, shown

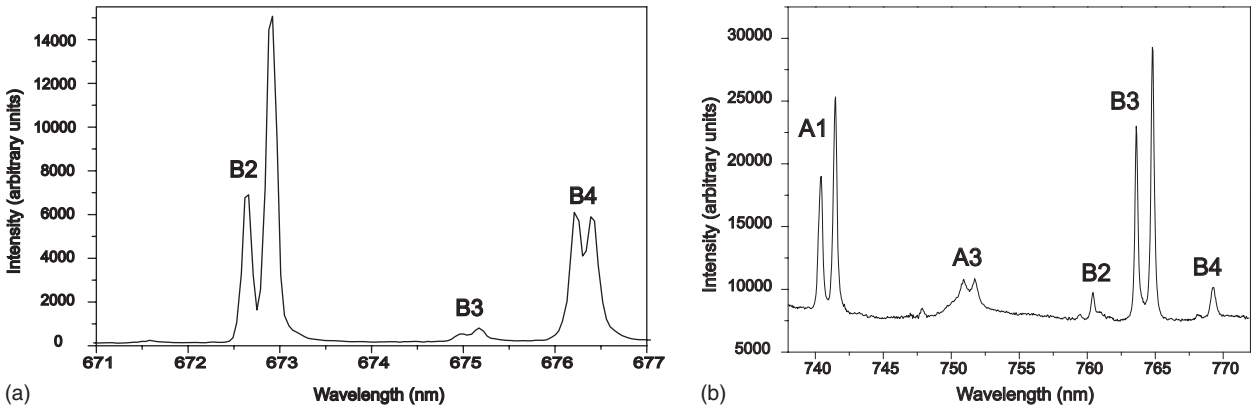

FIG. 10. Twofold stress-induced splittings of no-phonon lines observed with 488 nm excitation at ~7 K. (a) Splitting of the B2, B3, and B4 lines from a sample of 4*H*-SiC. (b) Splitting of the A1, A2, A3, B2, B3, and B4 lines from a sample of 6*H*-SiC.

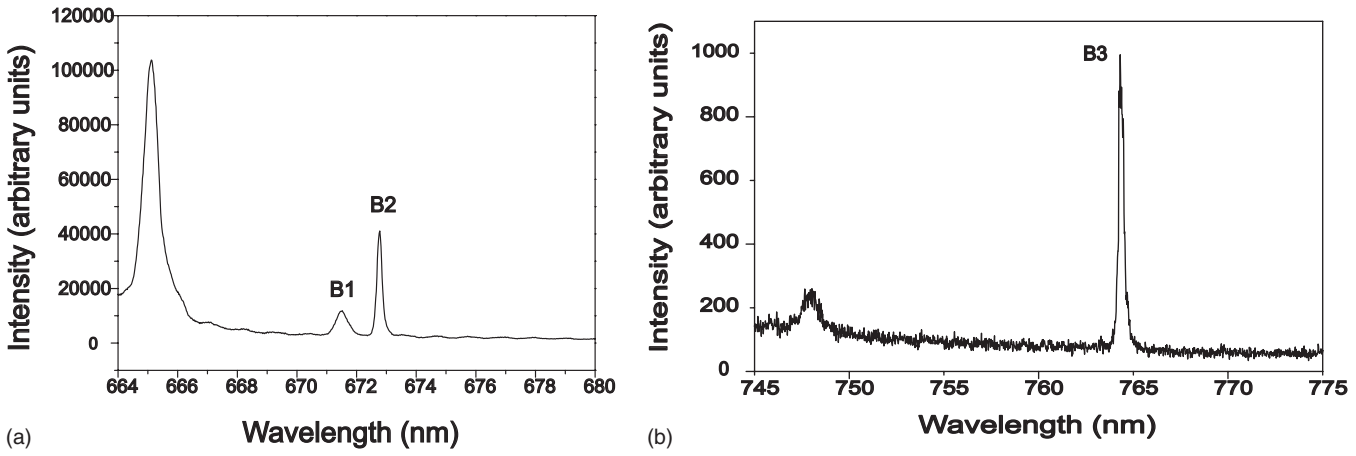

FIG. 12. Photoluminescence excitation spectra obtained at 2 K. (a) Excitation of the vibronic structure (750–780 nm) of B2 and B4 PL of 4*H*-SiC as the wavelength of the dye laser used for excitation was changed. (b) Excitation of the vibronic structure (770–830 nm) of B1-B4 PL of 6*H*-SiC as the wavelength of the Ti-sapphire laser used for excitation was changed.

in Fig. 12(b), were obtained with a Ti-sapphire laser. In this case resonant emission occurred at just two wavelengths (748.65 and 764.8 nm). The lack of a third resonant excitation at a slightly shorter wavelength than 764.8 nm is consistent with the lack of temperature dependence of the relative intensities of the B1-B4 PL. It is notable that the 748.65 nm resonance for 6*H*-SiC was weak in comparison with that at 664.7 nm for 4*H*-SiC. By studying, with 488 nm excitation, the PL spectra of both polytypes at about 150 K, emission was detected at the resonant excitation wavelengths 667.4 nm (4*H*) and 748.65 nm (1.656 eV-6*H*) revealed by the excitation spectra.

F. Formation conditions for A and B centers in 4*H*-SiC

A single simple condition, based on the results of the low-temperature PL spectra, has been found to be remarkably effective in determining whether a 4*H*-SiC sample will exhibit AB or V behavior after room-temperature electron irradiation. If the sample lacks DAP emission, independent of its *p* or *n* nature and its doping level, it will generally be V type but if there is relatively strong DAP emission then it will be AB type. Exceptions to this simple rule occurred for the high-purity semi-insulating sample studied here, and for the samples with comparable peak intensities of N and DAP emission as was the case for the bulk-grown samples. The marked differences between the AB and V materials will now be summarized.

Typical characteristics of AB material in 4*H*-SiC were that the AB PL completely dominated the 488 nm excited spectra to such an extent that the laser power level was sometimes reduced to avoid detector saturation. There were generally only a few weak additional ZPLs in the spectra. Strong AB spectra were encountered after room-temperature irradiation at doses down to 10^{17} e cm^{-2} although a low-temperature anneal at 250 °C was necessary to produce the spectrum after irradiation at this dosage. It was also produced, with lower intensity, after room-temperature irradiation and subsequent annealing at 400 °C for low electron energies down to 130 keV to a dose of 10^{20} e cm^{-2}. There was no discontinuous change on dropping to voltages below the Si displacement threshold (250 keV).[13] For material irradiated at 750 °C, AB PL was present for electron energies down to 110 keV. In all cases the A and B PL were produced together in the same intensity ratios and the peaks annealed out together maintaining the same intensity ratios. The AB PL intensities were enhanced after room-temperature irradiation for all doses by annealing at about 400 °C and for the higher doses, in excess of 10^{19} e cm^{-2}, the peaks were found at large distances outside the electron irradiated regions after this annealing treatment; they could often be easily detected more than 100 μm beyond the perimeter of the irradiated zone. Figure 13 illustrates the B2 intensity distribution across an irradiated region in comparison with that of the (comparatively weak) V_1 emission from a sample where both emissions occurred. The AB centers in this type of material were

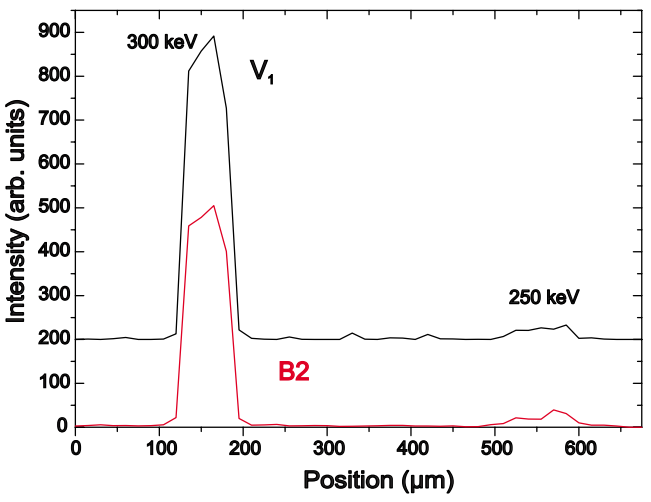

FIG. 13. (Color online) Spatial distribution of intensity for V_1 emission (weak, *x*6) and B2 emission for a high-intensity AB sample from which both emissions were detected. The irradiation was in a circular region of 200 μm diameter to a dose of 10^{19} e cm^{-2} and the sample was annealed at 600 °C. 488 nm excitation at ~7 K.

quite stable on annealing, generally surviving 1100 °C anneals and they were sometimes still present after annealing at 1300 °C. AB samples with epilayers were studied edge-on under confocal optical conditions and it was found that the underlying substrates made an even greater contribution to the AB emission, generally having an intensity about twice that of the epilayers. On the basis of a few experiments it was found that for incidence of 130 keV electrons normal to the C face of AB samples, including samples for which this was the growth face, differences were detected. Relatively few such irradiations have been performed but the evidence indicates that the formation of the AB centers is inhibited under these conditions. However, for 300 keV irradiations on the C face of these samples no differences were detected.

The behavior of V material was very different and, surprisingly, hardly depended on the *n* or *p* character of the material or on the doping level. After room-temperature irradiation, with 300 keV electrons to a dose of 10^{19}–10^{20} e cm^{-2}, the 488 nm excited spectrum had several significant ZPLs in addition to V_1 but no AB PL. The most prominent of these was a pair of lines of remarkably narrow linewidth having several high-energy local vibrational modes. These ZPLs, at 640.5 and 672.3 nm, have been discussed previously[14] but lack an atomic model for their origin. They annealed out at 300–400 °C and, after somewhat higher annealing temperatures, a variety of other ZPLs of approximately comparable but relatively low intensity appeared. Many of these additional centers were the subject of a previous publication[15] but they include AB PL. The first evidence of AB PL appeared after annealing at 600 °C and its intensity grew progressively as the annealing temperature was raised to 950 °C. This growth of intensity was accompanied by decrease in V_1 intensity that finally vanished at 950 °C. The maximum intensities of AB PL ultimately achieved in this category of material were much lower than those observed for the AB material and they did not survive an 1100 °C anneal. For V material the AB PL was mainly restricted to the irradiated region itself, independent of dose, as illustrated in Fig. 14. However, there was a subtle distinction between the *p*- and *n*-doped materials which in other respects behaved similarly. Whereas the AB PL was entirely restricted to the irradiated regions for *n*-type samples for *p*-type material, after annealing at 900 °C, very weak AB PL could be detected at considerable distances outside it (see Fig. 15). Unlike AB material, the AB PL was only observed in samples irradiated with electrons having energies above the Si displacement threshold and for high electron doses. It has not been observed for electron energies below 250 keV or for doses of 10^{18} e cm^{-2} or below. Irradiations performed at 750 °C produced modestly enhanced AB intensity compared with 950 °C annealed room-temperature irradiations. The only detected difference for the most highly doped *n*-or *p*-type samples was a reduced rate of defect introduction. All samples studied edge-on revealed that the AB PL came only from the epilayers without any substrate contribution. All the materials listed in Tables I and II behaved in a similar way apart from the high-purity semi-insulating sample in Table I. Its PL spectrum revealed N-bound exciton luminescence without DAP emission but it exhibited predominantly AB characteristics with some V_1 emission as well.

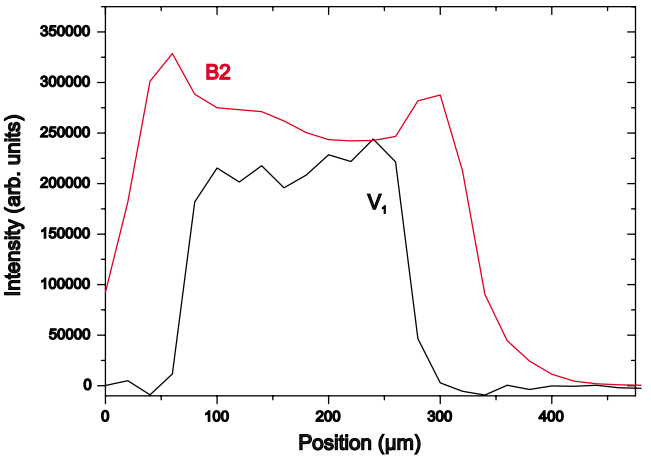

FIG. 14. (Color online) Spatial distribution of intensity for V_1 emission and B2 emission at ~7 K for a high-V sample irradiated in two displaced circular regions of 100 μm diameter to a dose of 10^{20} e cm^{-2} and subsequently annealed at 875 °C. The step length was 15 μm and the circular irradiated regions were 100 μm in diameter. The region on the left of the figure was irradiated at 300 keV, that on the right at 250 keV. The spectra are displaced vertically for clarity.

A few irradiations of AB and V materials were made at 1 MeV. At this voltage the AB PL was not normally present even in AB material until the samples were annealed but there was very strong V_1 PL. When the AB PL appeared, after annealing, its spatial distribution was similar to that described for the 300 keV irradiated material.

The final category to be discussed is the bulk material. This exhibited variable behavior, sometimes predominantly AB but without spreading outside the irradiated region, sometimes with V_1 and AB PL of comparable intensity.

Similar distinctions between different types of 6*H* material have not been found but the range of samples studied was limited to bulk grown or substrate material, all relatively highly doped and impure, and the irradiations that have been performed at higher or lower temperatures are fewer.

Experiments have also been performed with localized implantation of energetic light ions to see if there were parallels

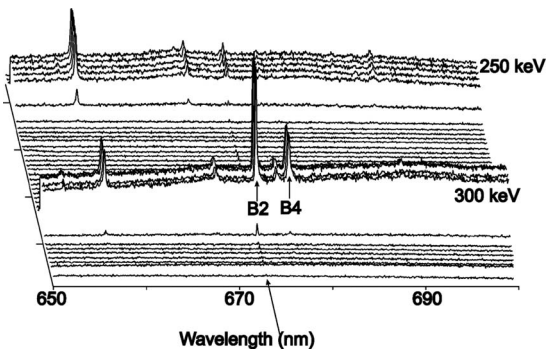

FIG. 15. Line scan of spectra generated at ~7 K, after annealing a 4*H* *p*-type V sample at 950 °C, by stepping a 488 nm laser probe across two separated regions of electron irradiation at the energies indicated. The spectra are staggered slightly for clarity. The arrow indicates the line of very weak B2 emission from regions well outside of the irradiated areas.

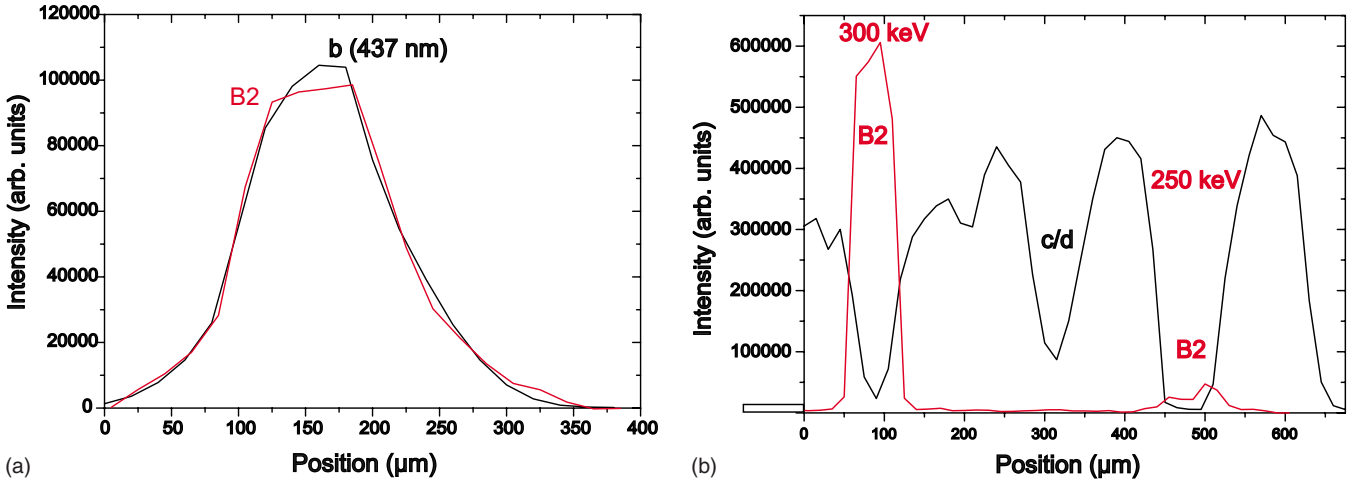

FIG. 16. (Color online) Spatial distributions of intensity (a) for *b* and B2 emission from an AB sample irradiated in a circular region of 100 μm diameter to a dose of 2×10^{19} e cm^{-2} and subsequently annealed at 400 °C; (b) for *c*/*d* from a V sample irradiated in two displaced circular regions of 100 μm diameter to doses of 10^{20} e cm^{-2} after annealing at 400 °C and for B2 emission after annealing 875 °C. The region on the left of (b) was irradiated at 300 keV, that on the right at 250 keV. All the spectra were generated at a temperature ~7 K. The *c*/*d* spectra from which (b) was derived were obtained with 325 nm excitation; the other spectra were obtained with 488 nm excitation [using the second order of the grating for *b* in (a)].

with the results of electron irradiation (see Ref. 16 for a preliminary report). AB PL was detected in V material implanted with 5 μm diameter 1 MeV He or proton beams in the regions peripheral to the implantations. After annealing at 900 °C the spatial spreading of the AB PL became much more extensive and its intensity distribution resembled that of the *a*-*d* lines prior to annealing. Close to the periphery of the implanted regions twofold splitting of the ZPLs occurred and the surface of the implanted regions was found to be dimpled. Sometimes spallation of material in these regions occurred after a delay of some weeks.

A very interesting comparison involves the spatial distributions of the so-called[8] *b*-*d* alphabet lines (the *a* lines have different spatial distributions of intensity). In both categories of material, for similar doses, these extended similar distances outside of the irradiated areas and after doses ~10^{20} e cm^{-2} there was considerable intensity at distances of 100 μm away from their perimeters. For AB material the B2 and *b*-*d* line distributions were always very similar [Fig. 16(a)] but for V material the B2 and *b*-*d* distributions were quite different with *b*-*d* extending large distances outside but B2 being almost entirely restricted to the irradiated region itself [Fig. 16(b)]. The spatial distributions of the intensities of the *b*-*d* lines were similar in both categories of material for similar doses, with *b*, *c*, and *d* extending large distances outside the irradiated regions [Figs. 16(a) and 16(b)].

G. Conditions of observation

Nearly all the observations reported here were made using 488 nm laser excitation. It was not generally possible to detect the AB PL using 325 nm excitation although it was occasionally detected as very weak broad peaks after long exposure times. More interesting are the results obtained using 785 nm laser excitation. At this wavelength the AB PL was not excited but the excitation of V_1 emission was greatly enhanced and samples in which no V_1 emission was detected with 488 nm excitation were found to emit it quite strongly. It is apparent that the AB centers, when present, rob the V_1 centers of excitation.

IV. DISCUSSION OF RESULTS

The absence or near absence of V_{Si}-related PL from the samples of AB material irradiated at 300 keV apparently points to an obvious explanation for the AB PL. Si atoms must have been displaced because the electron energy was above the Si displacement threshold [~250 keV (Ref. 13)], and damage certainly occurred because of the existence of strong alphabet line intensity, similar to that obtained from V materials after the same dose. As the only intense PL from the AB material, other than the alphabet lines, is that of AB PL the implication is that this is where the Si vacancies have gone. There are several experimental results that lead to this conclusion and we will summarize these before dealing with the factors that control the formation of V_CC_{Si} pairs.

First, the twofold splitting of the ZPLs in the ^{13}C enriched samples of 6*H*-SiC is of particular significance. There was a similar but smaller splitting in the case of the 4*H* polytype. Unlike the stress-induced effect, also described, this splitting was constant in magnitude in each region studied and did not vary with the laser position. Moreover, the relative intensities of the two lines depended on the ^{13}C concentration in the material, the shorter wavelength line decreasing in intensity for samples with reduced ^{13}C concentration. The clear and unambiguous conclusion from these observations is that there is just one C atom involved in the centers. Second, there is strong evidence that the centers involve a vacancy. The rapid broadening of the ZPLs as their intensities increased is behavior typical of vacancy-related centers as is also the associated relatively strong vibronic coupling and the lack of high-energy local vibrational modes. The

vacancy-related nature of the defects is also consistent with the unusually large isotope-related splitting in the 6*H* polytype so that the various individual contributions to the effect[17] are enhanced by its relatively soft nature. The isotopic splitting of the Si-vacancy defect in diamond is a related example.[18] These two crucial observations together with the formation of AB PL in AB samples irradiated at electron energies far below the Si displacement threshold so that only C vacancies can be involved are clear evidence for the identification of the defect with $V_C C_{Si}$ pairs. However, there is strong supporting evidence.

Samples containing various concentrations of $V_C C_{Si}^+$, $V_C C_{Si}^-$, and Si-vacancy-related centers, as determined by electron paramagnetic resonance studies in Tsukuba, were kindly provided by Dr. Umeda. AB PL was observed in both the *p*- and *n*-doped samples where electron paramagnetic resonance indicated $V_C C_{Si}^+$ and $V_C C_{Si}^-$, respectively, and strong V_1 PL in the sample that gave strong Si vacancy-related electron paramagnetic resonance. C vacancies are ruled out because the existence of AB PL at large distances outside the irradiated regions [Figs. 13 and 16(b)] is incompatible with the anticipated lack of C-vacancy mobility at the temperatures involved. The characteristic asymmetrical shape of the ZPLs was resolved into a weak satellite to B2 as illustrated in the inset to Fig. 2 and it was previously speculated[11] that this might result from next-nearest-neighbor pairs. Finally, the enhanced AB emission after high-temperature irradiations (750 °C) of samples in both categories, but more particularly in the less pure category, is consistent with the previously reported enhanced production of $V_C C_{Si}^-$ at this temperature.[2]

It is already well established by *ab initio* calculations that the energy barrier to formation of $V_C C_{Si}$ pairs from Si vacancies is small in *p*-type material[1,4] and by experiments that it is promoted by increase in the irradiation temperature.[2] We now discuss the experimental evidence that the formation of the AB centers is, in fact, facilitated by several additional factors including the impurity content, the electron energy and the dose so that the defect can also be formed in *n*-type materials and even for electron energies below the Si-vacancy creation threshold in some *p*-type materials.

The profiles of the AB lines in 4*H*-SiC were dependent on the sample purity and the dose. Both for high impurity levels, as in material exhibiting strong DAP PL, and high doses, these profiles broadened markedly. Similar behavior was observed for the increase in V_1 linewidth with dose in V material but did not occur for the previously studied C antisite-related complexes that involve interstitial atoms.[3,19] This well-known effect is a consequence of inhomogeneous nanoscale electric and strain fields acting on relatively soft defects. The DAP PL exhibited by the samples listed in Table III indicates that the donor and acceptor atoms exist at sites only a few atomic positions apart whereas, even at a doping level of 10^{17} cm^{-2}, the dopant sites in the uncompensated material are about 100 atom spacings apart. In addition, the results obtained from ion-implanted V material provide direct evidence for a completely independent source of long-range internal stress that also has important consequences for the electron irradiated material. Nomarski interference optical microscopy performed on the surface of the implanted samples revealed the presence of surface dimples in the locally implanted regions and in some cases the related stresses were sufficiently high to cause spallation of SiC. Spallation from electron-irradiated regions has also been observed on rare occasions. These stresses, generated by the high concentrations of defects created, are relatively long-range, dose-dependent, and add to the above-mentioned inhomogeneous stresses that are a consequence of the sample purity and defect density.

The temperature of irradiation was also found to be an important factor, reduction in temperature favoring V_1 formation, raising it favoring the formation of AB centers. Two major issues to address are the remarkably similar AB behavior of *n*- and *p*-type V category material but the equally remarkably different behavior of AB and V material with the same *p*-doping levels. These results appear to be in direct conflict with theoretical work[4] that shows the barrier to transformation from V_{Si} to $V_C C_{Si}$ pairs is doping dependent, favored in *p*-type material but inhibited in *n*-type material. In the case of the V material one possibility is that the Fermi level of these materials becomes pinned in a midgap position as a consequence of irradiation. There is direct evidence for irradiation-induced carrier freeze out in the case of the 10^{16}–10^{17} cm^{-3} *n*-doped samples. In its unirradiated state, the highest energy LO line observed in Raman studies was appropriately broadened and shifted to higher wave number.[20] However, after irradiation, the peak sharpened and returned to smaller wave numbers, by a dose-dependent amount, as a result of a reduction in electron concentration with lowering of the Fermi level. While the argument of midgap pinning might be relevant for the low-doped samples it is hard to reconcile for the similar behavior of the highly doped samples. In order to account for the similarity of the behavior of the *n*- and *p*-type V samples and also for the different behavior of the similarly *p*-doped AB and V material it is evident that there must be additional mechanisms in operation. A more satisfactory argument relies on consideration of the influence of pre-existing and irradiation-induced stress fields and electric fields together with the effect of temperature rise in overcoming the barrier to $V_C C_{Si}$ pair formation. In V material the AB PL is largely restricted to the irradiated region itself, where the defect related stress is greatest. Moreover, it is necessary to create Si vacancies, to employ a high electron dose and, after room-temperature irradiation, to anneal at temperatures of 600 °C or above to achieve AB PL in it. We argue that here the combination of high stresses and temperatures are sufficient to transform Si vacancies into $V_C C_{Si}$ pairs in the irradiated region. In the case of AB materials, the high concentrations of donors and acceptors mean that inbuilt nanoscale stresses and electric fields exist prior to irradiation. On irradiation the nanoscale fields are supplemented by longer range fields generated by the defects introduced. There is direct experimental evidence for the existence of these fields from the large linewidths of the AB no-phonon lines. Consequently there is introduction of AB centers in the irradiated regions of high-dose samples without annealing although more are created with thermal assistance. However, it is necessary to explain how this can happen in material irradiated with electrons of much lower energy than is required to create Si vacancies. A clue to the

explanation of this behavior may lie in the observation that on annealing this material the AB intensity distribution matches that of the *b*-*d* alphabet lines and for high doses this extends well outside the irradiated region itself as illustrated in Fig. 16(a). Since the proposed explanation for the AB centers involves C antisites and the *a*-*d* lines are believed to result from antisite pairs[21] the experimental results could be explained if it is possible to find a low-energy route for Si antisite loss to occur. The available evidence indicates that as the AB centers increase in intensity on annealing AB material the *a*-*d* lines simultaneously decrease in intensity and at the same time other colocated centers appear that have local vibrational modes of relatively low energy, perhaps consistent with Si-interstitial-related centers. One of these centers has a ZPL at 396.6 nm and a rather low-local vibrational mode energy of 157.3 meV (Ref. 22) (the three higher energy modes given in this reference have since been found to be sum modes of lower energy vibrations). The second has a ZPL at 414.2 nm and a very low-LVM energy of 129.2 meV.[15] Even if no such mechanism can be found it should be noted that the *b*-*d* lines, involving C antisites, exist at large distances from highly irradiated regions just like the V_CC_{Si} centers. The lack of AB PL in high-dose 1 MeV as-irradiated AB material may be explained by the removal of C antisites from the antisite/vacancy pairs by the higher energy electrons creating nearest-neighbor divacancies.

There remains one further relevant observation to discuss. After annealing in the temperature range 800–950 °C very weak B2 and B4 PL could be detected at large distances outside the irradiated regions of *p* doped but not *n*-doped V material (it is too weak to be visible in Fig. 14 but can be seen in Fig. 15). This is the temperature range in which the 325 nm PL results show that the *b*-*d* lines were annealed out. As the Fermi level will be pinned by the doping type at locations far from the irradiated region we conclude that the thermal assistance in the *p*-type material was just sufficient to create AB centers from these alphabet lines whereas this was not the case for *n*-doped material.

In the discussion so far we have restricted our comments to the results for the 4*H* polytype. There are some obvious parallels with the results from 6*H*-SiC. Both materials have A and B sets of lines. The two A lines for 4*H*-SiC become three for 6*H*-SiC. The PLE experiments reveal just one fundamental B line for each polytype but stress splits this into two lines for 4*H*-SiC but three for 6*H*-SiC. The A and B lines for both materials have similar polarization properties (with some differences of detail). In particular, the main emission lines, B2 for 4*H*-SiC and B3 for 6*H*-SiC, were both strongly polarized perpendicular to [0001] but for 6*H*-SiC the B3 line was only strongly excited if the laser was similarly polarized. There are however marked differences of formation and annealing behavior. For 4*H*-SiC the ratio of the intensities of the A set to the B set was remarkably constant and they annealed out together at rather high temperatures. For 6*H*-SiC the B lines were always in approximately the same intensity ratio and they annealed out at a similar high temperature to the 4*H* A and B lines. However, the relative intensities of the three A lines varied considerably and so did their overall intensities relative to the B set. Moreover, the A lines annealed out at considerably lower temperatures (600–800 °C) than the B lines. Finally, the individual B lines in 6*H*-SiC maintained their relative intensities on increasing the sample temperature while in the 4*H* material the B2 line had a nearby excited state of slightly higher energy causing the B2 and B4 lines to become four as the sample temperature was raised.

In 4*H*-SiC there are two slightly different on-axis pairs, one pseudocubic the other pseudohexagonal, as well as two different mixed pseudocubic/pseudohexagonal off-axis pairs. As the on-axis pairs have, in principle, higher symmetry than the off-axis pairs and their epr results are distinct[2] it is reasonable to suppose that one pair produces the A lines and the other B. In 6*H*-SiC there are three distinct on-axis and three off-axis pairs. The fact that the B lines are more intense than the A lines for the 4*H*-SiC might indicate that they correspond to the off-axis cases since there are three of these for each on axis configuration. The effect of stress on the centers will be to introduce additional asymmetry leading to differences in the configurations of the on-axis and off-axis defects and hence to additional energy levels. In particular, the three equivalent configurations of the off axis defects need no longer be identical under stress.

Another issue involves a comparison of the observed optical properties of the centers with the results of existing *ab initio* calculations for the V_CC_{Si} center. Unfortunately, the calculations are limited at present to the negative charge states of the axial V_CC_{Si} defect, and were performed in connection with epr experiments.[23] We are not able to determine the charge states of the AB centers directly but the evidence presented here indicates that the defects we have studied were in a neutral state and, in particular, the failure to detect either splitting or shift of the lines in 12T magnetic fields is consistent with zero spin and hence this deduction. An AB type *p*-doped sample with DAP emission that was irradiated with 1.5 MeV electrons to a dose of 10^{18} e cm^{-2} and annealed to produce strong AB PL was studied by electron paramagnetic resonance by Ms Dhaenens-Johansson at the University of Warwick. She found V_C^+ centers but no $V_CC_{Si}^+$ centers. The conclusion of neutrality of the defects is supported by the relatively long life-time of the B2 emission (0.27 μs) and by the scaling of its emission energies with the bandgaps of 4*H*- and 6*H*-SiC which together indicate isoelectronic character. Further supporting evidence comes from the PL experiments on samples provided by Dr. Umeda and studied by epr in Tsukuba. We found AB PL in both the *n*-type and *p*-type samples although the Tsukuba experiments found them, respectively, in the negative and positive charge states. Moreover, the AB PL showed no intensity discontinuity on warming above 50 K (Fig. 3) although the epr results from the $V_CC_{Si}^-$ centers exhibited a marked discontinuity. This discontinuity has been interpreted as occurring because a low-temperature low-symmetry state of the negatively charged defect has its symmetry raised when a static Jahn-Teller distortion becomes dynamic.[1] The neutral state of the defect is not expected to have a Jahn-Teller distortion.[24] The combined experimental information from the PL and PLE experiments on the B center of 4*H*-SiC can be summarized by the energy-level diagrams in Fig. 17. For 4*H*-SiC we know from the *ab initio* calculations that the *e* ground state of the $V_CC_{Si}^-$ center is split into two *a* states by the Jahn-

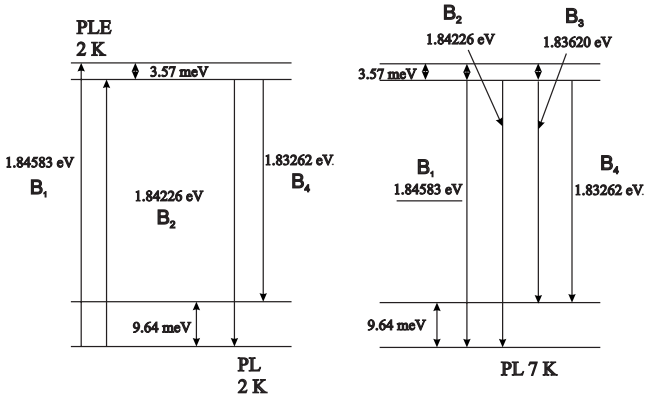

FIG. 17. Energy-level diagrams that are consistent with the data obtained from the PL and PLE experiments reported in the text. The underlined energies on the right of the figure are thermally excited transitions.

Teller effect[23] and this is consistent with the diagram. Also, the observed emission energies are not very different from the rather approximate energies derived from these calculations (~1.1 eV) for on-axis pairs. We are not able, at present, to account for the B2 and (very weak) B1 lines of 6*H*-SiC with an energy-level diagram. However, in this connection, it may be relevant that only for this polytype did the intensities of the B-line spectrum depend on the polarization direction of the incident laser beam suggesting that in this case the excitation process was chiefly directly between defect energy levels and it is notable that the resonant 748.65 nm excitation was relatively weak. The resonant 665 nm excitation of B PL in 4*H*-SiC has not been included on the energy-level diagram because of its breadth, possibly indicating excitation via the conduction band which would be consistent with the independence of the results of polarization experiments on the polarization direction of the incident laser beam.

We next summarize the different annealing behaviors observed in the two categories of materials. For V material the PL of the as-irradiated material revealed C-interstitial-related alphabet lines, dicarbon antisites $(C_2)_{Si}$ (Ref. 3) and V_1 PL. C vacancies are not detected by PL but epr evidence has shown that they are stable to high temperatures. On annealing, the AB PL began to appear at 600 °C and it grew in intensity up to an annealing temperature of 950 °C. In this temperature range the alphabet lines started to decrease in intensity and by 900 °C both the *b*-*d* alphabet lines and the V_1 PL had been eliminated. As the only significant internal stress in this material was limited to the irradiated region it is consistent with our arguments that the only significant AB PL intensity appeared there. This evidence appears to indicate that at least some of the Si vacancies were converted into the V_CC_{Si} defects but the situation is not clear because it is well-known several distinct mechanisms can contribute to this loss.[25] At about 900 °C the $(C_2)_{Si}$ PL is replaced by dicarbon antisite pairs $[(C_2)_{Si}]_2$ and then at higher temperatures (~1300 °C) these are replaced by tricarbon antisites $(C_3)_{Si}$.[19] At higher temperatures still D1 PL becomes the dominant component of the PL spectrum. The PL mentioned above as possibly related to Si interstitials started to appear at 900 °C and annealed out by 1400 °C. The chief difference between this behavior and that of the AB material is that while the AB PL in V material is eliminated by annealing at 1100 °C it may still be present in AB material after annealing at 1300 °C.

A remaining question concerns the mechanism that causes the long-range outward migration of certain atomic defects from the irradiated regions. It had previously been proposed that internal electric fields generated during the irradiation process were causing an outflow of charge that became trapped on mobile C_i defects and the subsequent neutralization of the charged C_i acted as a driving force for further outwards migration.[26] Eberlein *et al.*[27] brought forward an argument to account for the formation of Si_C from mobile C_i defects that involves charged defect states. Two other contributions to the outward migration are also possible. One is the inhomogeneous stress, generated in both AB and V material by the buildup of high densities of defects after high-dose irradiation. As judged by the alphabet-line intensity distributions, the outward migration occurs to a similar extent in both the AB and the V samples. The other is the generation of near-band-gap luminescence created by the recombining carriers in the highly excited region during irradiation, and its subsequent reabsorption at remote locations, regenerating carriers that drive the outward migrations further outwards. It should be noted that the potential for creation of thermally rather stable V_CC_{Si} centers at large distances from implanted regions could have important implications for the fabrication of devices from the material.

V. CONCLUSIONS

The evidence presented here leads to the conclusion that the A and B PL systems observed in electron irradiated or ion-implanted 4*H*- and 6*H*-SiC originate from neutral V_CC_{Si} centers. It is argued that the step of overcoming the relatively weak energy barrier to the formation of this defect from others introduced by electron irradiation is facilitated by the existence of internal stress fields and electric fields that are both pre-existing and also the result of irradiation damage as well as by raised temperature and the Fermi level position. The pre-existing fields in highly compensated material (AB) are responsible for the very different behavior of uncompensated material (V). We have produced evidence that suggests the formation of $(V_CC_{Si})^0$ results from transformation of Si vacancies, at least in part, in V material but it is clear that there must be a completely different additional route in the AB material. The similarity between the intensity distributions of the *b*, *c* and *d* alphabet prior to annealing and the AB intensity distributions after these alphabet lines have annealed out has led us to propose that this is a pointer to a separate transformation route. The distinction between AB and V material can be very important because the annealing properties of the V_CC_{Si} centers and of Si vacancies are quite different, the former generally stable to annealing temperatures of 1100–1300 °C while the latter generally anneal out in the temperature range 600–900 °C. In addition, the extent to which these defects are created outside the irradiated or implanted regions can differ greatly between the two catego-

ries. The sequence of defects subsequently created at higher temperatures is also likely to be significantly different.

The association of the A and B systems with on-axis and off-axis pairs remains uncertain at present but with the detailed information presented in this work, which includes an energy-level diagram for the B lines in 4*H*-SiC, it could probably be resolved by *ab initio* calculations.

Note added in proof. The 1.5 MeV electron-irradiated sample with a large number of AB centers has been found to exhibit strong UD-2 (Refs. 1 and 2) emission in low temperature infrared PL by J. P. David (Sheffield).

ACKNOWLEDGMENTS

This work would not have been possible without the willing and expert assistance of many people. Samples were kindly provided by G. Wagner (IKZ Berlin), F. la Via (ST Catania), P. Bergman (University of Linköping), P. Friedrichs (SiCrystal), T. Umeda (University of Tsukuba), W. N. Wang (Bath University), P. Wellmann (University of Erlangen), L. Ley (University of Erlangen), M. Uren (QINETIQ), and N. Wright (University of Newcastle). Experiments on high voltage TEMs were performed by F. Phillipp (Stuttgart, Max-Planck Institut für Metallforschung) and Cheng Yu Song (NCEM Berkeley USA). Ion implantations were performed by N. Peng (University of Surrey, Ion Beam Centre). High-temperature annealing was performed by students of N. Wright (University of Newcastle). PLE experiments were performed by A. Batalov and P. Siyushev (University of Stuttgart). U. d'Haenens-Johansson made epr and absorption measurement on one sample. Time-resolved (Bristol) and high magnetic field measurements (at the High Field Facility Grenoble) were performed by J. Hayes. A. Sarua assisted the interpretation of the Raman data. A. Gali, G. Davies, and Umeda made several helpful comments on the interpretation of the PL results. The initial experimental work on aspects of this investigation was performed by G. Evans, S. Charles, S. Furkert, and W. Sullivan as part of their work. The TEM irradiations in Bristol would not have been possible without the expert assistance of R. Vincent. Partial support was provided by the UK Engineering and Physical Science Research Council and by the Leverhulme Trust.

[1] M. Bockstedte, A Gali, A. Mattausch, O. Pankratov, and J. W. Steeds, Phys. Status Solidi B **245**, 1281 (2008).
[2] J. Isoya, T. Umeda, N. Mizuochi, N. T. Son, E. Janzén, and T. Oshima, Phys. Status Solidi B **245**, 1298 (2008).
[3] J. W. Steeds, W. Sullivan, S. A. Furkert, G. A. Evans, and P. J. Wellmann, Phys. Rev. B **77**, 195203 (2008).
[4] E. Rauls, T. Lingner, Z. Hajnal, S. Greulich-Weber, T. Frauenheim, and J. M. Spaeth, Phys. Status Solidi B **245**, R1 (2000).
[5] J. W. Steeds, W. Sullivan, A. Wotherspoon, and J. M. Hayes, J. Phys.: Condens. Matter **21**, 364219 (2009).
[6] I. G. Ivanov, B. Magnusson, and E. Janzén, Phys. Rev. B **67**, 165211 (2003).
[7] M. Wagner, N. Q. Thinh, N. T. Son, W. M. Chen, E. Janzén, P. G. Baranov, E. N. Mokhov, C. Hallin, and J. L. Lindström, Phys. Rev. B **66**, 155214 (2002).
[8] T. Egilsson, A. Henry, I. G. Ivanov, J. L. Lindstrőm, and E. Janzén, Phys. Rev. B **59**, 8008 (1999). The alphabet line descriptions *a*, *b*, *c*, or *d* lines have been used as abbreviations, for convenience. In fact, each "line" is a small family of two or four related lines, the higher energy lines resulting from thermally occupied states.
[9] E. Sörman, N. T. Son, W. M. Chen, O. Kordina, C. Hallin, and E. Janzén, Phys. Rev. B **61**, 2613 (2000).
[10] M. Wagner, B. Magnusson, W. M. Chen, E. Janzén, E. Sörman, C. Hallin, and J. L. Lindstrom, Phys. Rev. B **62**, 16555 (2000).
[11] J. W. Steeds, Mater. Sci. Forum **600-603**, 437 (2007).
[12] C. A. Arguello, D. L. Rousseau, and S. P. S. Porto, Phys. Rev. **181**, 1351 (1969).
[13] J. W. Steeds, F. Carosella, G. A. Evans, M. M. Ismail, L. R. Danks, and W. Voegeli, Mater. Sci. Forum **353-356**, 381 (2001).
[14] J. W. Steeds, S. Furkert, J. M. Hayes, and W. Sullivan, Mater. Sci. Forum **457-460**, 637 (2004).
[15] J. W. Steeds and W. Sullivan, Phys. Rev. B **77**, 195204 (2008).
[16] J. W. Steeds, N. Peng, and W. Sullivan, Mater. Sci. Forum **615-617**, 409 (2009).
[17] S. Hayama, G. Davies, J. Tan, J. Coutinho, R. Jones, and K. M. Itoh, Phys. Rev. B **70**, 035202 (2004).
[18] C. D. Clark, H. Kanda, I. Kiflawi, and G. Sittas, Phys. Rev. B **51**, 16681 (1995).
[19] A. Mattausch, M. Bockstedte, O. Pankratov, J. W. Steeds, S. Furkert, J. M. Hayes, W. Sullivan, and N. G. Wright, Phys. Rev. B **73**, 161201(R) (2006).
[20] T. Kitamura, S. Nakashima, T. Kato, and H. Okamura, Mater. Sci. Forum **600-603**, 501 (2009).
[21] T. A. G. Eberlein, R. Jones, S. Öberg, and P. R. Briddon, Phys. Rev. B **74**, 144106 (2006).
[22] J. W. Steeds, S. A. Furkert, W. Sullivan, J. M. Hayes, and N. G. Wright, Mater. Sci. Forum **483-485**, 347 (2004).
[23] T. Umeda, N. T. Son, J. Isoya, E. Janzén, T. Ohshima, N. Morishita, H. Itoh, A. Gali, and M. Bockstedte, Phys. Rev. Lett. **96**, 145501 (2006).
[24] A. Gali (private communication).
[25] M. Bockstedte, A. Mattausch, and O. Pankratov, Phys. Rev. B **69**, 235202 (2004).
[26] J. W. Steeds, G. A. Evans, L. R. Danks, S. Furkert, W. Voegeli, M. M. Ismail, and F. Carosella, Diamond Relat. Mater. **11**, 1923 (2002).
[27] T. A. G. Eberlein, C. J. Fall, R. Jones, P. R. Briddon, and S. Öberg, Phys. Rev. B **65**, 184108 (2002).